Combust. Sci. and Tech., 182: 1735–1746, 2010

ISSN: 0010-2202 print/1563-521X online
DOI: 10.1080/00102202.2010.497404

NUMERICAL AND EXPERIMENTAL INVESTIGATION OF DETONATION INITIATION IN PROFILED TUBES

Ilya V. Semenov,[1] Pavel S. Utkin,[1] Vladimir V. Markov,[2] Sergey M. Frolov,[3] and Victor S. Aksenov[4]
[1]*Institute for Computer Aided Design, Russian Academy of Sciences, Moscow, Russia*
[2]*V.A. Steklov Mathematical Institute, Russian Academy of Sciences, Moscow, Russia*
[3]*N.N. Semenov Institute of Chemical Physics, Russian Academy of Sciences, Moscow, Russia*
[4]*Moscow Engineering Physics Institute (State University), Moscow, Russia*

Detonation initiation in a tube with parabolic contraction and conical expansion was investigated numerically and experimentally. The optimized geometry of conical expansion with sine-shaped wall is proposed. The generalized diagram in the form of detonation curves at the contraction slope angle versus incident shock Mach number plane is presented. For solving the governing Euler equations, the numerical method based on finite volume approach with Godunov flux approximation adapted for multiprocessor systems is used. It has been shown experimentally that the parabolic contraction and conical expansion ensure shock-to-detonation transition in a stoichiometric propane-air mixture under normal conditions at a very low minimal incident shock wave velocity of 680 ± 20 m/s, which approximately corresponds to a Mach number of 2. This result is important for novel jet propulsion systems with detonative burning of fuel-pulse detonation engines.

Keywords: Detonation initiation; Experiment; Numerical modeling; Pulse detonation engine

INTRODUCTION

The interest to the problem of detonation initiation in tubes has recently increased in view of the development of pulse detonation engines (PDEs; Frolov, 2006; Roy et al., 2004). The most of relevant studies focus on detonation initiation by classical means, namely, direct detonation initiation by concentrated energy deposition (e.g., Lee, 1977; Levin et al., 2005; Sedov et al., 1988) and deflagration-to-detonation transition (e.g., Oran and Gamezo, 2007; Shchelkin 1949). It is known that for hydrocarbon-air mixtures the former requires large initiation energies whereas the latter requires long run-up distances. The energy and tube length requirements depend on tube diameter: the smaller the diameter the lower energy

Received 15 October 2009; revised 30 March 2010; accepted 2 April 2010.
Address correspondence to Ilya V. Semenov, Institute for Computer Aided Design, Russian Academy of Sciences, 123056, Moscow, Russia. E-mail: semenov@icad.org.ru

and shorter distance are required for detonation initiation. The conventional way of detonation initiation in a PDE channel is to transition a detonation from a small-diameter tube (predetonator) through various transition devices to a detonation chamber. Once initiated in the predetonator, a detonation can be transitioned to a tube of larger diameter by conical expansions (Borisov et al., 1991), disk-shaped obstacles (Murray et al., 2001), perforated plates (Vasiliev, 2006), or by combined means such as conical expansions with obstacles in the form of orifice plates (Marelli et al., 2005).

The other possible approach for detonation initiation in a PDE tube is shock-to-detonation transition (SDT). According to this approach, a relatively weak incident shock wave (ISW) propagating along the PDE tube can be effectively transitioned to a detonation using properly tuned distributed external energy sources (Frolov, 2005), tube coils (Frolov et al., 2005), tube bends (Frolov et al., 2007a), or tubes with regular shaped obstacles (Frolov et al., 2007b).

The numerical investigation of SDT in tubes with shaped obstacles was continued by Semenov et al. (2008a). The mechanism of SDT in a round tube with a localized parabolic contraction of the cross section followed by the conical expansion with smooth walls was analyzed qualitatively and quantitatively. Three stages of the SDT phenomenon have been identified, namely, (a) double Mach reflection of the ISW from the curved wall, (b) local explosion(s) due to the cumulation of Mach stem or reflected shock wave, and (c) detonation reinitiation due to interactions of blast waves from local explosions with the conical expansion (Semenov et al., 2008a, Semenov et al., 2009).

In this article we present the results of further computational and experimental studies aimed at the optimization of the conical expansion part of the shaped obstacle transitioning a relatively weak ISW to a detonation in the stoichiometric propane-air mixture.

COMPUTATIONAL STUDY

The round tube of diameter D comprises three sections: Section 1 with constant cross-section, Section 2 with a shaped contraction-expansion, and outlet Section 3 with constant cross-section (Figure 1). Initially, the tube is filled with the homogeneous, quiescent, stoichiometric propane-air mixture under normal conditions. The wall profile in Section 2 is given by the parabolic curve $z(r)$. The parabolic shape

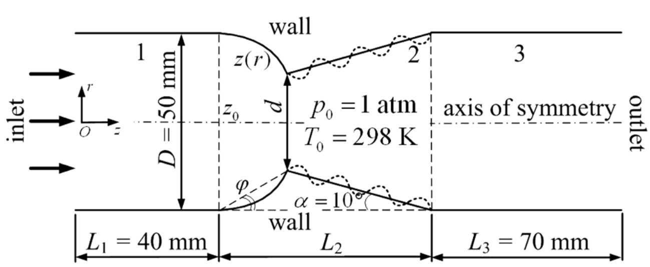

Figure 1 Statement of the problem.

$z(r)$ is chosen to meet the following constraints: (a) the focus of the parabola lies in the free stream at the tube symmetry axis; (b) the blockage ratio of contraction, $BR = 1 - (d/D)^2$, does not exceed a certain maximum value; and (c) angle ϕ does not exceed a certain limiting value. Twelve different values of angle ϕ ranging from 5° to 90° and three values of BR were investigated.

The problem is solved using symmetry conditions at the tube axis, slip condition at the walls, and zero-gradient outflow condition at the right boundary (see Figure 1). At time zero, the ISW of Mach number M and constant postshock flow is assumed to enter the computational domain through the inlet.

The mathematical statement of the problem is based on the set of equations for the axisymmetric, two-dimensional, transient flow of inviscid, compressible, multicomponent, explosive gaseous mixture. Propane oxidation is modeled by a single-stage overall reaction

$$C_3H_8 + 5O_2 + 19N_2 = 3CO_2 + 4H_2O + 19N_2 + Q,$$

where $Q = 46,6\,\text{KJ/g}$ is propane specific heat of combustion.

The number of the mixture components is $N = 5$: C_3H_8 ($i = 1$), O_2 ($i = 2$), N_2 ($i = 3$), CO_2 ($i = 4$), H_2O ($i = 5$). The rate of propane density change is determined as

$$\dot{\omega}_1 = \mu_1 \dot{\omega}_1^{mole} = \mu_1 \left(k \frac{\rho_1}{\mu_1} \cdot \frac{\rho_2}{\mu_2} \right),$$
$$k = -7 \cdot 10^{14} p^{-0.2264} \exp(-E^*/RT)\text{cm}^3/(\text{mole} \cdot \text{s}),\ E^* = 190,3\,\text{KJ/mole},$$

where $\dot{\omega}_1^{mole}$ is the rate of first component, propane-molar concentration change, p is pressure in atmospheres, and T is temperature in Kelvin degrees. The reaction kinetics was obtained by fitting the predicted and measured ignition delays (Frolov et al. 2007a).

The numerical procedure for solving Euler equations is based on splitting the physical processes and on the finite volume approach with the explicit time integration scheme and second-order Godunov scheme for fluxes. The numerical algorithm for parallel computing is used (see Semenov et al., 2008b). The spatial resolution is 0.05–0.1 mm, whereas the time resolution is 10 ns.

As a result of numerical simulation of ISW transition through the contraction with various values of ϕ, BR, and ISW Mach number, the curves shown in Figure 2 were plotted for the case with smooth conical expansion. At $BR = 0.75$, the curve exhibits a pronounced minimum at $M = 2.65$ and $\phi = 45°$. The grater M, the broader the interval of ϕ where SDT is observed in the calculations. In view of the fact that at $\phi = 45°$ SDT is always obtained at $M > 2.65$, this shape is referred to as optimal for $BR = 0.75$. It is this shape that has been chosen for experimental validation. The existence of optimal shape is discussed by Semenov et al. (2009) in detail.

To optimize the shape of the conical expansion (case $BR = 0.75$), the expansion with wavy (sine-shaped) wall was considered (dotted curve in Figure 1). Such wall pattern is determined by the number of sine periods along the expansion length and sine amplitude.

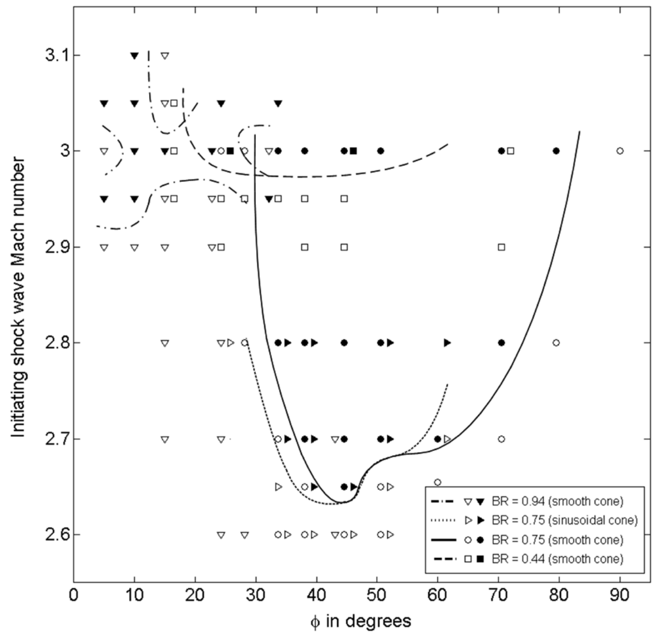

Figure 2 Detonation curves: open symbols = SDT no go, closed symbols = SDT go conditions.

In all calculations with SDT, the tube length was $z^* = L_1 + L_2 + L_3$. The length of the outlet section L_3 was chosen equal to 70 mm to be sure that the detonation is either initiated or not for a certain geometry of shaped walls with minimal CPU time requirements (see Figure 1). However, numerical experiments with $L_3 > 70$ mm were also performed to check the validity of findings for $L_3 = 70$ mm (see Figures 3a and 3b for $L_3 = 140$ mm). The same applies to the case of SDT failure (see Figures 3c and 3d).

The mechanism of detonation initiation in the tube with parabolic contraction and conical expansion (see Semenov et al., 2008a; Semenov et al., 2009) implies that if DW fails to form at cross section z^* a reasonable increase of L_3 will not change the situation. Thus, Figure 3 shows the failure of detonation initiation in a tube with the smooth-walled conical expansion while the sinusoidal shaping of the conical expansion leads to detonation initiation, other conditions being equal. In the calculations, the detonation regime was detected based on (a) tracing the lead SW velocity along the tube axis (see Figure 4a) and (b) by means of numerical soot footprints (i.e., recording the pressure maxima during the whole computational run [see Figure 4b] caused by the multifront DW structure). The averaged velocity of the self-sustained detonation in the calculations was 2040 m/s. This value exceeds the Chapman-Jouguet velocity for the stoichiometric propane-air mixture at normal conditions, 1800 m/s (Vasilev, 2008), but very close to the theoretical Chapman-Jouguet velocity of 2050 m/s determined for the reaction products of the single-stage kinetic model in use.

Consider the mechanism of detonation initiation for the case of sine-shaped conical expansion at $M = 2.65$, $\phi = 38°$, and $BR = 0.75$ (see Figures 3a and 3b). Figure 5 indicates that at 88 μs the first and the second deepenings of the sinusoidal conical

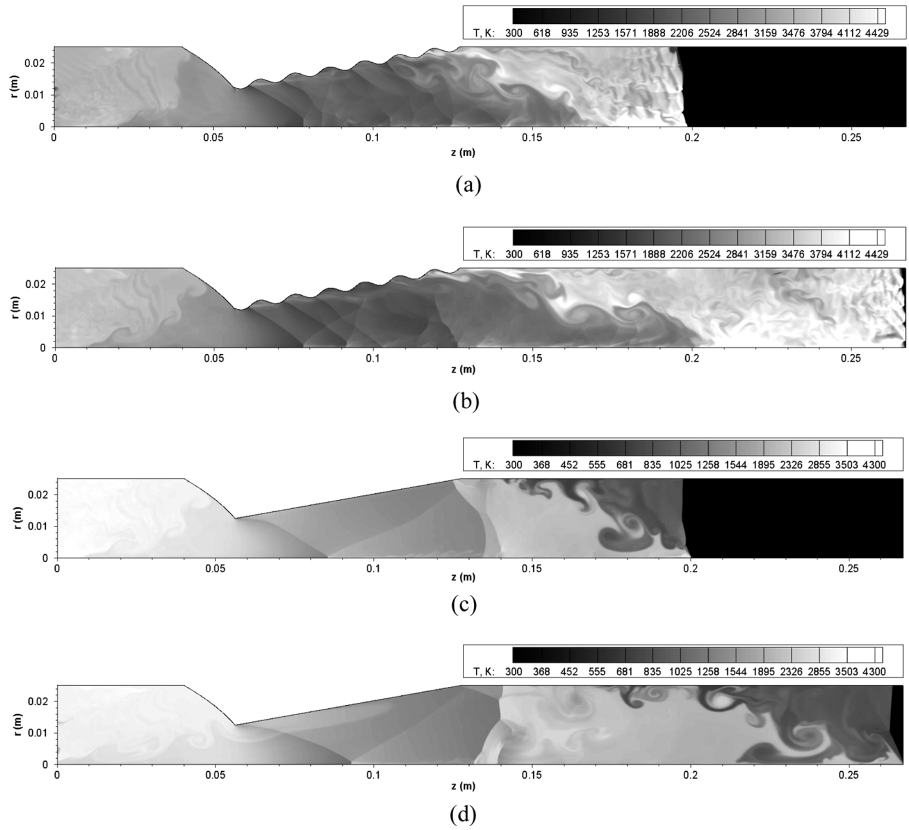

Figure 3 DW propagation in a tube with parabolic contraction and sinusoidal conic expansion for $M = 2.65$, $\phi = 38°$, $BR = 0.75$ at (a) 148 µs and (b) 182 µs. Detonation initiation failure in a tube with parabolic contraction and smooth conic expansion under the same conditions at (c) 184 µs and (d) 240 µs. Predicted fields of temperature (in K).

surface appear to get filled with the preheated explosive mixture in front of the blast wave from the local explosion at the tube axis. This preheating is caused by multiple reflections of the leading shock wave and secondary waves from the sine-shaped wall (see the snapshot corresponding to 94 µs). As a result, in the course of blast wave propagation along the wall, successive autoignitions occur followed by local explosions in the deepenings located downstream. The autoignition regions first appear at 88 µs. The next autoignition occurs at 96 µs. Each local explosion leads to the formation of a blast wave propagating through the combustion products towards the tube axis and to the DW moving in the fresh mixture along the wall. The snapshot corresponding to 100 µs demonstrates the temporal detonation decay. However the third local explosion (104 µs) leads to the formation of the DW that occupies nearly the entire tube cross section. Such stage-by-stage amplification of the lead front results in SDT.

The sine-shaped conical expansion provides the results somewhat similar to those obtained experimentally with traveling ignition pulses (Frolov, 2005): a local explosion in each subsequent deepening plays the role of a successive igniter.

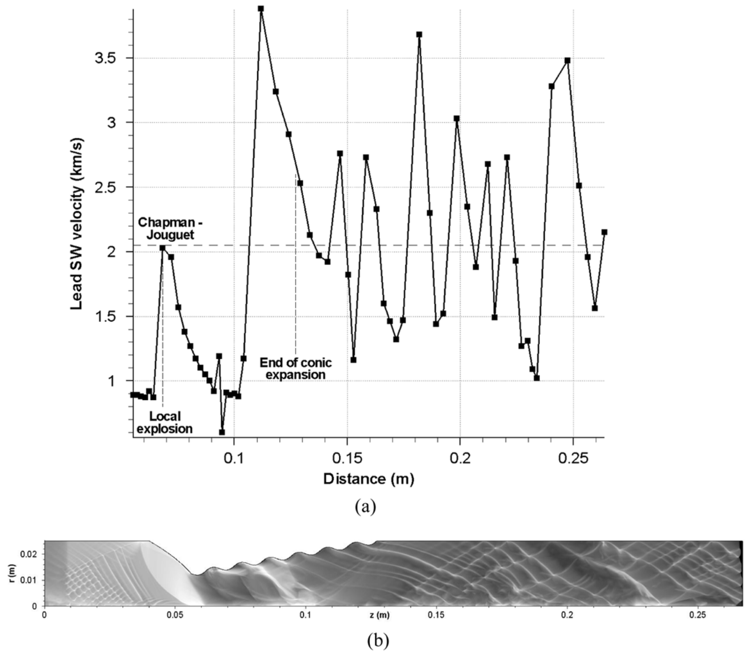

Figure 4 (a) Calculated leading shock wave velocity at the tube axis of symmetry versus distance and (b) numerical soot footprints in case of detonation initiation in a tube with parabolic contraction and sinusoidal conic expansion under conditions similar to those in Figure 3.

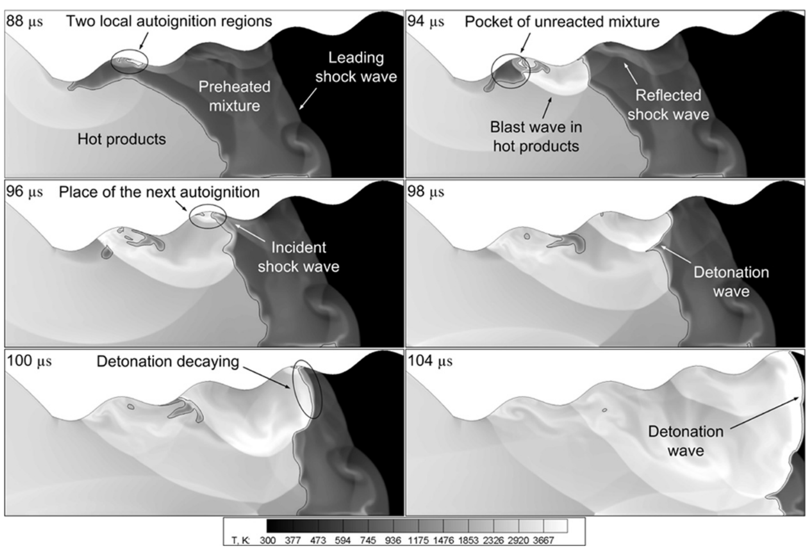

Figure 5 The mechanism of detonation initiation in a tube with parabolic contraction and sinusoidal conic expansion under conditions similar to those in Figure 3. Predicted fields of temperature (in K). The black lines are the isolines of propane concentration 1%.

The limiting conditions for SDT in the sine-shaped conical expansion differ from those for the smoothed-walled conical expansion (see Figure 2). At low values of ϕ the sine-shaped conical expansion promotes SDT whereas at high values of ϕ it does not. The failure of detonation initiation at $M=2.7$, $\phi=60°$, $BR=0.75$ in the case of sinusoidal expansion is caused by the expansion of hot combustion products from local explosion thus preventing further propagation of the DW along the wall.

EXPERIMENTAL STUDY

The experiments were carried out in a 4500 mm long straight round tube 52 mm in diameter (Figure 6) with the stoichiometric propane-air mixture. Before each experiment, the tube was evacuated and then filled with the mixture until normal initial conditions (temperature = 293 ± 2 K, pressure = 1 atm). The ISW was produced by a solid-propellant gas generator, which was a cylindrical combustion chamber with a volume of 22 cm^3 equipped with a changeable bursting diaphragm with an outlet orifice diameter of 6 mm and a T6000 piezoelectric pressure transducer (Figure 6, transducer PT1). The construction and performance of the gas generator was the same as in (Frolov et al., 2007a).

At a distance of 2100 mm from the orifice exit section of gas generator, a shaped obstacle (nozzle) consisting of a parabolic contraction and conical expansion was installed. The profile of the contraction section corresponded to the optimal profile in Figure 1 (without sine-shape surface modulation) with $\phi=45°$, BR = 0.75, and α taken equal to 10° or 3°. In the latter case, the length of the conical expansion was increased by a factor of about 3.2 as compared to the computational example. The pressure and ISW velocity profiles were recorded with LKh600 piezoelectric pressure transducers PT2–PT9.

The experimental procedure was the following (Frolov et al., 2006; Frolov et al., 2007a): A weighed (2–3 g) charge of 12/7 CA cotton powder was placed in the gas generator. The charge was ignited by a weighed sample (0.3 g) of porous cotton powder. The solid-propellant gas generator produced SW with a long compression phase duration: the time of outflow of propellant gases exceeded 1 ms. Diaphragms of various thicknesses from different materials allowed us to vary the maximal pressure in the gas generator and, hence, the ISW velocity.

Figure 7 shows the lead shock wave velocity at different measuring segments: PT1–PT2, PT2–PT3, PT3–PT4, PT4–PT5, PT5–PT6, PT6–PT7, PT7–PT8 and

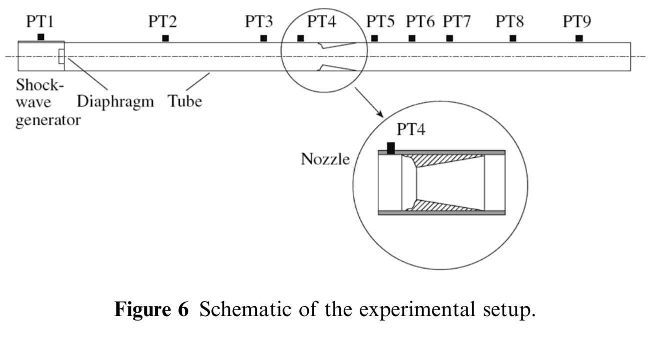

Figure 6 Schematic of the experimental setup.

PT8–PT9 in 8 representative experiments. The moment of diaphragm rupture was determined from the record of transducer PT1. The measuring segment PT1–PT2 corresponded to the distance between gas-generator and PT2 transducer (877 mm). The dashed vertical line (distance 2130 mm) in Figure 7 corresponds to the minimal cross section of the nozzle. The dashed horizontal line corresponds to the Chapman-Jouguet detonation velocity of 1800 m/s. The mean shock wave velocity at each measuring segment was determined based on the distance between the pressure transducers and the time taken for the shock wave to traverse this distance. The error of determining the shock wave velocity is estimated as 3%. Figure 7 shows that the SDT occurs when the ISW velocity exceeds a certain minimal (critical) velocity value. For the 52 mm diameter, 4500-mm long tube with the optimal shape of contraction–expansion, this critical velocity is equal to 970 ± 30 м/с. For the stoichiometric propane-air mixture this velocity corresponds to the SW Mach number of $M \approx 2.85$. This value is close to that predicted by the numerical simulation ($M \approx 2.65$). Note that at $M < 2.85$, the pressure histories at transducers PT5–PT8 indicate the existence of strong secondary blast waves behind the lead shock wave. The detonation arising behind the obstacle seems to decay due to relatively sharp conical expansion with $\alpha = 10°$. Therefore further experiments were made with cone expansion angle $\alpha = 3°$.

Figure 8 presents the results of ten representative experiments for the conical expansion with $\alpha = 3°$ other conditions being equal. Again, the vertical dashed line (at 2130 mm) shows the position of the minimal nozzle cross-section and the upper dotted line represents the Chapman-Jouguet detonation velocity (1800 m/s). Similar to Figure 7, Figure 8 indicates that there is a certain minimal (critical) value of the average velocity of the ISW at the contraction inlet at which detonation is initiated in the tube (i.e., the SDT is a threshold phenomenon). The critical value for the 52 mm diameter, 4500-mm long tube with the optimal shape of contraction but with 3°

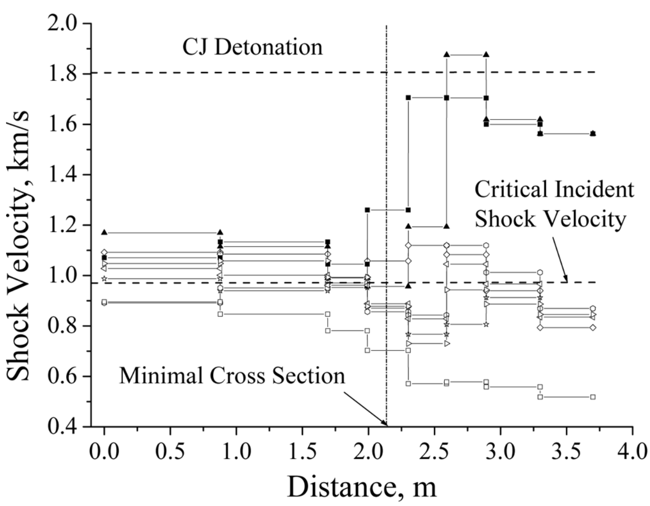

Figure 7 Average velocity of leading shock wave front versus traveled distance in various measuring segments in 8 representative experiments in the setup with $\phi = 45°$, $BR = 0.75$, and $\alpha = 10°$.

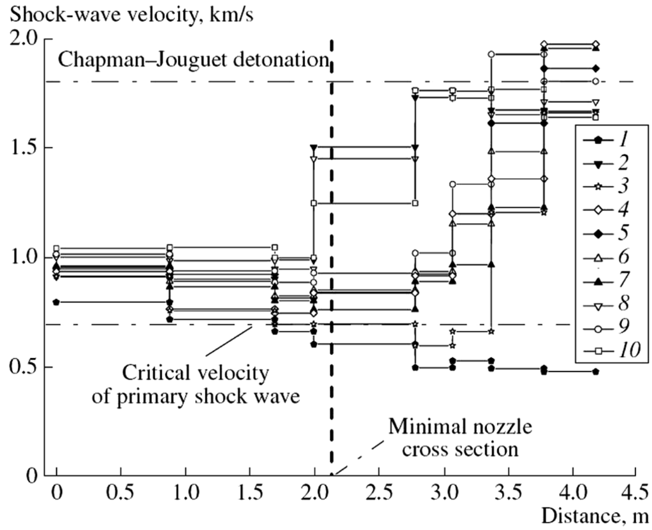

Figure 8 Average velocity of leading shock wave front versus traveled distance in various measuring segments in 10 representative experiments in the setup with $\phi = 45°$, $BR = 0.75$, and $\alpha = 3°$.

conical expansion appeared to be $680 \pm 20\,\mathrm{m/s}$. For the stoichiometric propane-air mixture under normal conditions, this velocity corresponds to a Mach number of approximately 2. If the average shock wave velocity at the nozzle inlet is below this critical value, there is no detonation (Figure 8, Experiment 1). If the average SW velocity at the nozzle inlet is above this critical value, there is SDT (Figure 8, Experiment 2–10) with no detonation decay in the conical expansion and downstream of it.

Figure 9 presents the pressure records by pressure transducers PT2–PT9 with identification of wave phenomena in one of the experiments with detonation initiation (Experiment 9). The average shock wave velocity at the contraction inlet is $890 \pm 30\,\mathrm{m/s}$. Transducers PT8 and PT9 detect detonation propagating at velocities 1930 ± 60 and $1810 \pm 50\,\mathrm{m/s}$ in the measuring segments PT7–PT8 and PT8–PT9, respectively. The average shock wave velocity in the measuring segment PT8–PT9 is very close to the Chapman-Jouguet detonation velocity. Thus, in the experiment considered, the SDT occurred at a distance of approximately $3570 \pm 204\,\mathrm{mm}$ from the gas generator, or at a distance of $1440 \pm 204\,\mathrm{mm}$ from the minimal nozzle section and $990 \pm 204\,\mathrm{mm}$ from the outlet of the conical expansion.

Figure 10 presents the detonation run-up distance as a function of the average velocity of ISW at the contraction inlet. While drawing Figure 10, it was assumed that the detonation run-up distance is the distance to the point where the velocity of the leading shock wave reaches at least $1500 \pm 45\,\mathrm{m/s}$. With an increase in the average velocity of the ISW, the detonation run-up distance is seen to decrease. At an average velocity of the ISW above 950–1000 m/s, detonation occurs within the conical expansion. This fact seems important for designing the process in PDEs. Unlike conventional notions that a nozzle is intended for controlling the outflow of detonation products and for enhancing the specific impulse of PDE, in this case, the

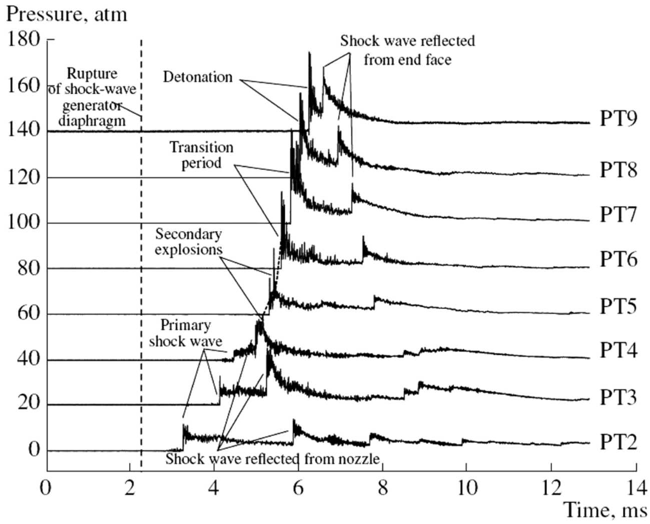

Figure 9 Pressure records of transducers PT2–PT9 in Experiment 9 with identification of wave phenomena.

nozzle is designed for both initiating detonation and controlling the outflow of explosion products.

The experimental studies of sine-shaped modulation of the nozzle expansion wall are presently underway and are aimed at decreasing the critical ISW velocity required for the detonation onset inside the nozzle.

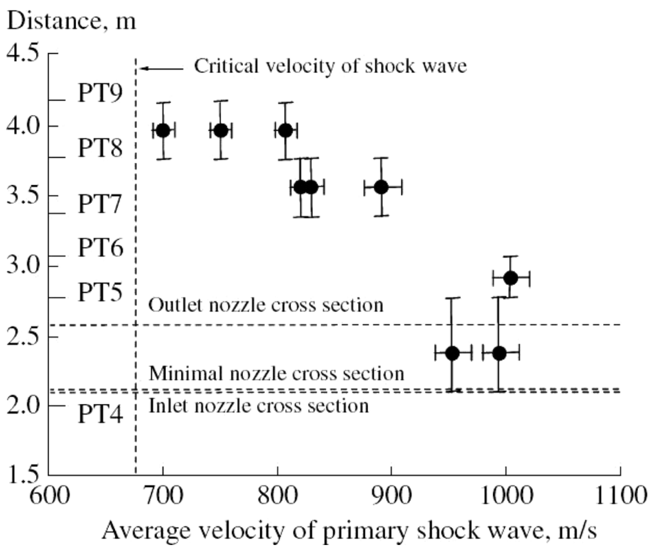

Figure 10 Detonation run-up distance versus average velocity of ISW at the nozzle inlet.

CONCLUSION

The computational and experimental studies of SDT in round tubes with a contraction–expansion have been performed. It has been shown numerically that the proper shaping of the contraction results in the detonation curve at the contraction slope angle versus ISW Mach number plane. The sinusoidal shaping of conical expansion can either promote SDT or lead to detonation initiation failure. The mechanism of successful SDT is revealed. The experimental studies, in general, confirmed the numerical findings regarding SDT in tubes with parabolic contraction and smooth-walled conical expansion. The nozzle of optimal geometry with the conical expansion angle $\alpha = 10^\circ$ was shown to provide SDT at $M \geq 2.85$ but the arising detonation had a tendency to decay in the course of propagation downstream the conical expansion. The decrease of the expansion angle to $\alpha = 3^\circ$ resulted in SDT at $M \geq 2$ and self-sustained detonation propagation. Note that such a shock wave is easy to produce (e.g., by replacing the solid-propellant gas generator and a portion of the tube upstream the nozzle in the experimental setup by a tube section with a Shchelkin spiral). After ignition of the explosive mixture by a weak heat source, the flame acceleration in the section with the Shchelkin spiral gives rise to a shock wave propagating at a velocity of 900–1000 m/s (Frolov et al., 2005).

ACKNOWLEDGMENTS

This work was supported by Russian Foundation for Basic Research (grant 08–08-00068) and Special Purpose Program of Russian Federation, Scientific and Educational Human Resources of Innovative Russia (contracts P359 and P502).

REFERENCES

Borisov, A.A., Khomik, S.V., Mikhalkin, V.R., and Saneev, E.V. 1991. Critical energy of direct detonation initiation in gaseous mixtures. In Kuhl, A.L., Leyer, J.C., Borisov, A.A., and Sirignano, W.A. (Eds.) *Dynamics of Detonations and Explosions*, Progr. Astron. Aeron. Ser., AIAA Inc., Washington, DC, Vol. 133, pp. 142–155.

Frolov, S.M. 2005. Initiation of strong reactive shocks and detonation by traveling ignition pulses. *Journal of Loss Prevention*, **19**, 238–244.

Frolov, S.M. 2006. *Pulse Detonation Engines*, Torus-Press, Moscow.

Frolov, S.M., Aksenov, V.S., and Basevich, V.Y. 2005. Decreasing the predetonation distance in a drop explosive mixture by combined means. *Dokl. Phys. Chem.*, **401**, 28–31.

Frolov, S.M., Aksenov, V.S., and Basevich, V.Y. 2006. Shock-to-detonation transition due to the shock interaction with the zone of prechamber jet ignition. *Dokl. Phys. Chem.*, **410**, 255–259.

Frolov, S.M., Aksenov, V.S., and Shamshin, I.O. 2007a. Shock wave and detonation propagation through U-bend tubes. *Proc. Combust. Inst.*, **31**, 2421–2428.

Frolov, S.M., Semenov, I.V., Komissarov, P.V., Utkin, P.S., and Markov, V.V. 2007b. Reduction of the deflagration-to-detonation transition distance and time in a tube with regular shaped obstacles. *Dokl. Phys. Chem.*, **415**, 209–213.

Lee, J.H.S. 1977. Initiation of gaseous detonation. *Ann. Rev. Phys. Chem.*, **28**, 75–104.

Levin, V.A., Markov, V.V., and Zhuravskaya, T.A. 2005. Nonlinear wave processes that occur during the initiation and propagation of gaseous detonation. *Proc. of the Steklov Inst. of Mathematics*, **251**, 200–214.

Marelli, A., Khasainov, B., Guilly, V., Presles, H.-N., and Desbordes, D. 2005. Promoting detonation diffraction from circular tube to cone by obstacles. *Proc. 20th ICDERS*, CD, Paper No. 25.

Murray, S.B., Thibault, P.A., Zhang, F., Bjerketvedt, D., Sulmistras, A., Thomas, G.O., Jenssen, A., and Moen, I.O. 2001. The role of energy distribution on the transmission of detonation. In Roy, G., Frolov, S., Netzer, D., and Borisov, A. (Eds.) *High-Speed Deflagration and Detonation: Fundamentals and Control*, ELEX-KM, Moscow, pp. 139–162.

Oran, E.S., and Gamezo, V.N. (2007) Origins of the deflagration-to-detonation transition in gas-phase combustion. *Combustion and Flame*, **148**, 4–47.

Roy, G.D., Frolov, S.M., Borisov, A.A., and Netzer, D.W. 2004. Pulse detonation propulsion: Challenges, current status and future perspective. *Progress in Energy and Combustion Science*, **30**, 545–672.

Sedov, L.I., Korobeinikov, V.P., and Markov, V.V. 1988. The theory of propagation of blast waves. *Proc. of the Steklov Inst. of Mathematics*, **2**, 187–228.

Semenov, I.V., Utkin, P.S., and Markov, V.V. 2008a. Numerical modeling of two-dimensional flows with detonation waves using high performance computing. *Numerical Methods and Programming*, **9**, 119–128.

Semenov, I.V., Utkin, P.S., and Markov, V. 2008b. Numerical study of the influence of tube wall profile on shock-to-detonation transition. *Proc. 7th ISHPMIE*, **2**, 16–24.

Semenov, I.V., Utkin, P.S., and Markov, V. 2009. Numerical simulation of detonation initiation in a contoured tube. *Combustion, Explosion and Shock Waves*, **45**, 700–707.

Shchelkin, K.I. 1949. *Fast Combustion and Spin Detonation of Gases*, Moscow, Voenizdat.

Vasiliev, A.A. 2006. Outstanding problems of gaseous detonation. In Roy, G. and Frolov, S. (Eds.) *Pulse and Continuous Detonation Propulsion*, Torus Press, Moscow, pp. 3–20.

Vasiliev, A.A. 2008. Energy aspects of initiation of domestic gases. *Combustion, Explosion and Shock Waves*, **44**, 86–91.